Signal Transduction:

Ligands Raise the Constraint That Limits Constitutive Activation in G Protein-coupled Opioid Receptors

Vanessa Vezzi, H. Ongun Onaran, Paola Molinari, Remo Guerrini, Gianfranco Balboni, Girolamo Calò and Tommaso Costa

J. Biol. Chem. 2013, 288:23964-23978.
doi: 10.1074/jbc.M113.474452 originally published online July 8, 2013

THE JOURNAL OF BIOLOGICAL CHEMISTRY VOL. 288, NO. 33, pp. 23964–23978, August 16, 2013

Ligands Raise the Constraint That Limits Constitutive Activation in G Protein-coupled Opioid Receptors*[S]

Received for publication, April 4, 2013, and in revised form, July 2, 2013 Published, JBC Papers in Press, July 8, 2013, DOI 10.1074/jbc.M113.474452

Vanessa Vezzi[‡], H. Ongun Onaran[§], Paola Molinari[‡], Remo Guerrini[¶], Gianfranco Balboni[‖], Girolamo Calò[**], and Tommaso Costa[‡1]

*From the [‡]Department of Pharmacology, Istituto Superiore di Sanità, 00161 Rome, Italy, the [§]Molecular Biology and Technology Research and Development Unit, Department of Pharmacology, Faculty of Medicine, University of Ankara, 06100 Ankara, Turkey, the [¶]Department of Chemistry and Pharmaceutical Sciences, University of Ferrara, 44100 Ferrara, Italy, the [‖]Department of Life and Environment Sciences, University of Cagliari, 09124 Cagliari, Italy, and the **Department of Medical Sciences, University of Ferrara, 09124 Ferrara, Italy*

Background: Native subtypes of G protein-coupled receptors (GPCR) show different levels of constitutive activation.
Results: Using a BRET assay to detect receptor-G protein complexes, we find that constitutive activation causes a uniform reduction of the apparent efficacy of all ligands.
Conclusion: An intramolecular energy barrier separates constitutive from ligand-regulated activation.
Significance: The data suggest that GPCR activation involves both cooperative and anticooperative components.

Using a cell-free bioluminescence resonance energy transfer strategy we compared the levels of spontaneous and ligand-induced receptor-G protein coupling in δ (DOP) and μ (MOP) opioid receptors. In this assay GDP can suppress spontaneous coupling, thus allowing its quantification. The level of constitutive activity was 4–5 times greater at the DOP than at the MOP receptor. A series of opioid analogues with a common peptidomimetic scaffold displayed remarkable inversions of efficacy in the two receptors. Agonists that enhanced coupling above the low intrinsic level of the MOP receptor were inverse agonists in reducing the greater level of constitutive coupling of the DOP receptor. Yet the intrinsic activities of such ligands are identical when scaled over the GDP base line of both receptors. This pattern is in conflict with the predictions of the ternary complex model and the "two state" extensions. According to this theory, the order of spontaneous and ligand-induced coupling cannot be reversed if a shift of the equilibrium between active and inactive forms raises constitutive activation in one receptor type. We propose that constitutive activation results from a lessened intrinsic barrier that restrains spontaneous coupling. Any ligand, regardless of its efficacy, must enhance this constraint to stabilize the ligand-bound complexed form.

Mutant and occasionally wild-type forms of G protein-coupled receptors (GPCRs)[2] can exist in a state of constitutive (ligand-independent) activation. Some ligands show "negative efficacy" in reversing this spontaneously active state and are thus named inverse agonists or negative antagonists (1–4). Unraveling the mechanisms of constitutive activity is important for the understanding of the functional chemistry of receptors (5) and may suggest novel therapeutic interventions for several genetic diseases associated with naturally occurring constitutively active receptor mutations (6–12).

Constitutive activation and inverse agonism are quantitatively predictable on the basis of the theoretical background that describes the cooperative effects between two ligand binding processes (*i.e.* the ligand and the Gα subunit) taking place on distinct sites of the same protein (*i.e.* the receptor) (13–18). However, little additional progress has been made in unraveling the mechanism and the structure-activity relationships that underlie the phenomenon of receptor constitutive activation. At least two factors hamper progress in the field.

One is the difficulty of quantifying the extent of ligand-independent activity. Constitutive activation can be assessed as the difference in basal signaling between cells expressing or not expressing the receptor. The magnitude of this transfection-dependent signaling is very small, often at the lowest limit of signal detection, and requires subtracting two larger numbers (*i.e.* the "basal" signaling recorded in two different cell populations). Thus, quantitative biochemical assessment of negative efficacy is difficult to accomplish and varies widely across different studies.

The second problem is the rare availability of ligand congeners exhibiting gradual variations from positive to negative values of efficacy. Even when several inverse agonists are known for a given GPCR subtype, they often belong to a different chemical class than the agonist or the neutral antagonist. Thus, it is hard to evaluate how discrete modifications of structure may tune the transition from the positive to the negative region of efficacy (19).

Here we used a cell-free bioluminescence resonance energy transfer (BRET) assay of receptor-G protein interaction to

* This work was supported in part by Grant SBAG 110S 159 (to H. O. O.) from TÜBİTAK, the Scientific and Technological Research Council of Turkey.
[S] This article contains supplemental Table S1.
[1] To whom correspondence should be addressed: Istituto Superiore di Sanità, Dip. Farmaco, Viale Regina Elena 299, 00161 Roma, Italy. Tel.: 39-0649902386; E-mail: tomcosta@iss.it.
[2] The abbreviations used are: GPCR, G protein-coupled receptor; BRET, bioluminescence resonance energy transfer; MOP, μ-opioid; DOP, δ-opioid; FRC, fractional receptor-G protein coupling; IA, intrinsic activity; TCM, ternary complex model; Dmt, 2′,6′-dimethyl-L-tyrosine; Tic, 1,2,3,4-tetrahydroisoquinoline-3-carboxylate; DADLE, [D-Ala^2,D-Leu^5]enkephalin; GTPγS, guanosine 5′-3-*O*-(thio)triphosphate; BNTX, 7-benzylidenenaltrexone; Rluc, *Renilla* luciferase; ACM, allosteric complex model; ARM, allosteric receptor model; AGM, allosteric G protein model.

measure intrinsic and ligand-dependent coupling. In this system receptor binding to endogenous Gα subunits results in a reduced distance between the receptor C-terminal region and the N-terminal region of the $G\beta_1$ subunit. This causes enhanced resonance energy transfer emission between a bioluminescent (Rluc) donor and a fluorescent (*Renilla* GFP (RGFP)) acceptor that are genetically tethered to the respective endings of the two molecules (20–22). Binding of the guanine nucleotide to endogenous Gα subunits abolishes the signal, thus allowing measurement of the extent of constitutive activation as the difference in the basal signal between the absence and presence of GDP. We evaluated the differences in spontaneous and ligand-regulated coupling between μ (MOP) and δ (DOP) opioid receptors (23, 24), using 35 analogues that share a common peptidomimetic scaffold. This is derived from the condensation of the two unnatural amino acids, 2′,6′-dimethyltyrosine (Dmt) and 1,2,3,4-tetrahydroisoquinoline-3-carboxylic acid (Tic). As shown previously, substitutions within the Dmt-Tic pharmacophore can generate a vast array of changes in the affinity and efficacy of ligands for the two opioid receptors (25–28).

We found that more than 40% of the Dmt-Tic analogues studied displayed varying degrees of inverse efficacy for the DOP receptor but acted as partial or full agonists for the MOP receptor. This reversal of efficacy appears to depend on the greater constitutive activity of the DOP receptor compared with that of MOP. In fact, the maximal levels of absolute coupling for most ligands (*i.e.* the net BRET over the GDP base line) are remarkably similar at the two receptors. Analysis of the data suggests a new model of receptor constitutive activation. According to such a view, constitutive activation of the receptor results from the intramolecular lessening of a constraint that all ligands must oppose to stabilize the ligand-bound receptor-G protein complex.

EXPERIMENTAL PROCEDURES

Reagents and Drugs—Cell culture media, reagents, and fetal calf serum were from Invitrogen, restriction enzymes from New England Biolabs, coelenterazine and bisdeoxycoelenterazine from Biotium Inc., [D-Ala^2,D-Leu^5]enkephalin (DADLE) from Bachem, ICI-174,864 and BNTX from Tocris, and GDP (Tris salt) from Sigma-Aldrich. All DMT-Tic analogues were synthesized as reported (26–28). Their structures and abbreviations are listed in supplemental Table S1.

Cells and Membranes—The preparation of retroviral vectors coding for Rluc-tagged human MOP and DOP receptors and RGFP-fused Gβ1 or β-arrestin 2 and the transduction of SH-5YSY human neuroblastoma cells were described previously (22). Cells were grown in a 1:1 mixture of Dulbecco's modified Eagle's medium and F-12 with 10% (v/v) fetal calf serum, 100 μg/ml hygromycin B, and 400 μg/ml G418 in a humidified atmosphere of 5% CO_2 at 37 °C. Enriched membranes from transfected cells were obtained by differential centrifugation (22) and stored in aliquots at −80 °C before use.

BRET Measurement and Data Analysis—BRET signals were measured and analyzed as described previously (20–22). Receptor-$G\beta_1$ interactions were measured in 96-well white plastic plates (Packard Opti-plate) using membrane preparations (5 μg of protein) in a total volume of 100 μl of PBS; receptor-β-arrestin 2 interactions were measured in intact cell monolayers. All ligands were tested using 8 log-spaced concentrations, and in each assay microplate concentration-response curves for the nucleotide GDP and for the full agonist, DADLE, were included to assess, respectively, the level of zero and maximal receptor activation. At concentrations ≥ 100 μM several Dmt-Tic analogues produced detectable inhibition of Rluc activity (measured as in Ref. 22). Therefore, concentrations greater than 10 μM were avoided. Curves representing the change of BRET ratio as a function of ligand concentration were first analyzed by nonlinear curve fitting using the general logistic function (29), $BRET_{ratio} = d + (a - d)/[1 + (x/c)^{\pm b}]$ where x is ligand concentration, a and d are the curve asymptotes, c is the ligand concentration yielding half-maximal BRET change, and b is the slope factor at c (with positive or negative sign for agonists or inverse agonists and GDP).

Next, all data points were converted to fractional receptor-G protein coupling (FRC) by subtracting the maximal inhibition of BRET produced by GDP and dividing by the maximal stimulation induced by DADLE: $FRC = (BRET_{ratio} - d_{GDP})/(a_{DADLE} - d_{GDP})$, where d_{GDP} and a_{DADLE} are the best fitting parameters shared across the set of fitted curves and mark the 0 and 1 levels of coupling. Transformed data were refitted with the same equation to compute the ligands for intrinsic activity (IA, *i.e.* E_{max} in FRC units) and potency (EC_{50}, given as negative log value, pEC_{50}). Both parameters contain information about ligand efficacy (*i.e.* the intrinsic ability of each individual ligand to couple the system), but neither provides a simple proportional measure of it, as both are nonlinearly affected by the difference in binding affinity between the receptor and G protein. However, although potency also depends on the receptor binding affinity of the ligand, IA does not. The FRC in the absence of ligand is the level of spontaneous coupling of each empty receptor.

Concentration curves are shown as representative experiments (except where otherwise stated). The corresponding parameter values averaged from at least three independent experiments performed on membranes obtained from different batches of cells are shown in Tables 1 and 2.

RESULTS

Apparent Reversal of Ligand Efficacy in DOP and MOP Receptors—Ligand-mediated coupling between opioid receptors and $G\beta_1$ via endogenous Gα subunits was described previously (22). In this study we co-expressed each luminescent receptor with the fluorescent $G\beta_1$ subunit in the human neuroblastoma cells, SH-5YSY. The relative abundance of $G\alpha_o$ makes these cells a better model of the neuronal environment. Two lines expressing similar levels of receptors and $G\beta_1$ with virtually identical donor/acceptor ratios were selected for this study.

Using membrane preparations, we generated curves describing the change in FRC (see "Experimental Procedures") as a function of ligand concentration. The computed potencies (pEC_{50}) and IA of the 35 Dmt-Tic analogues are summarized in Table 1. An example of such concentration-response curves is shown in Fig. 1, *a* and *b*. Note the difference in spontaneous coupling between DOP and MOP receptors (Fig. 1, *shaded areas*). ICI-174,864 (prototypic inverse agonist) inhibited DOP receptor coupling to a level very close to the GDP base line but

TABLE 1

IA and potency (pEC_{50}) for Dmt-Tic ligand effect on FRC-Exp

E_{max}, indicates FRC observed at 10 μM. See supplemental Table S1 for ligand abbreviations and structures.

Ligand	DOP receptor			MOP receptor			
	IA (FRC ±S.E.)	pEC_{50} (-log±S.E.)	*n*	IA (FRC ±S.E.)	Exp. E_{max} (FRC ±S.E.)	pEC_{50} (-log±S.E.)	*n*
Empty receptor	0.48 (0.007)		12	0.09 (0.007)			12
DADLE	1.00 (0.018)	7.60 (0.071)	12	1.00 (0.039)		7.84 (0.035)	12
ICI 174,864	0.07 (0.013)	7.20 (0.032)	12	N.M.	0.43 (0.052)	<=4	9
Tic-Ala	0.34 (0.027)	8.31 (0.051)	3	N.M.	0.32 (0.036)	<=5	3
Tic-Asp	0.49 (0.017)	–	3	N.M.	0.54 (0.029)	<=5	3
Tic-Asn	0.25 (0.028)	7.92 (0.094)	3	N.M.	0.68 (0.021)	<=6	3
Tic-DAsn	0.27 (0.027)	8.04 (0.088)	3	N.M.	0.48 (0.087)	<=5	3
Tic-Glu	0.89 (0.009)	7.92 (0.081)	3	N.M.	0.30 (0.053)	<=5	3
Tic-DGlu	0.79 (0.010)	7.09 (0.127)	3	N.M.	0.26 (0.039)	<=4	3
Tic-Gln	0.31 (0.026)	8.35 (0.069)	3	N.M.	0.24 (0.039)	<=4	3
Tic-DGln	0.36 (0.026)	7.98 (0.139)	3	N.M.	0.37 (0.045)	<=5	3
Tic-Arg	0.81 (0.035)	6.63 (0.266)	3	0.76 (0.042)		6.36 (0.097)	3
Tic-Lys(Ac)	0.17 (0.025)	8.16 (0.146)	3	N.M.	0.26 (0.036)	<=5	3
Tic-DLys(Ac)	0.25 (0.026)	8.36 (0.063)	3	N.M.	0.65 (0.030)	<=6	3
Tic-Lys	0.48 (0.004)	–	3	0.74 (0.040)		6.07 (0.023)	3
Tic-Gly	0.63 (0.012)	7.18 (0.080)	3	N.M.	0.68 (0.029)	<=6	3
Tic-Ser	0.60 (0.026)	7.33 (0.385)	3	0.73 (0.030)		6.13 (0.056)	3
Bid-Bzl	0.71 (0.013)	7.19 (0.059)	3	0.84 (0.053)		7.03 (0.069)	3
Bid-Propen	0.59 (0.026)	7.52 (0.294)	3	0.85 (0.015)		7.56 (0.124)	3
Bid-cPropyl	0.61 (0.036)	6.81 (0.174)	3	0.86 (0.009)		7.36 (0.089)	3
UFP-512	0.91 (0.032)	8.95 (0.108)	3	0.83 (0.019)		7.63 (0.051)	3
UFP-502	0.90 (0.025)	8.08 (0.324)	3	0.82 (0.018)		7.93 (0.110)	3
dMeUFP-502	0.74 (0.024)	8.01 (0.377)	3	N.M.	0.20 (0.034)	<=6	3
C1-Bid	0.75 (0.024)	7.63 (0.301)	3	0.75 (0.030)		7.29 (0.076)	3
dMe-C1-Bid	0.36 (0.028)	8.90 (0.176)	3	0.19 (0.038)		6.55 (0.069)	3
Gly-Bid	0.64 (0.039)	7.86 (0.428)	3	0.71 (0.033)		6.90 (0.069)	3
dMe-Gly-Bid	0.15 (0.027)	8.49 (0.223)	3	0.09 (0.008)		7.40 (0.133)	3
Tib	0.81 (0.038)	8.14 (0.366)	3	0.89 (0.018)		7.40 (0.160)	3
dMe-Tib	0.40 (0.035)	8.62 (0.211)	3	0.38 (0.054)		6.67 (0.063)	3
Tic-Ph	0.70 (0.018)	8.11 (0.200)	3	0.95 (0.040)		7.52 (0.078)	3
dMe-Tic-Ph	0.28 (0.037)	8.66 (0.057)	3	0.52 (0.122)		6.25 (0.377)	3
Tic-Gly-Ph	0.84 (0.017)	8.58 (0.247)	3	0.93 (0.013)		8.21 (0.038)	3
dMe-Tic-Gly-Ph	0.23 (0.029)	8.61 (0.151)	3	0.24 (0.038)		7.31 (0.030)	3
UFP-505	0.60 (0.031)	7.71(0.523)	3	0.92 (0.012)		7.71 (0.061)	3
dMe-UFP-505	0.12 (0.020)	8.46(0.199)	3	0.23 (0.039)		7.39 (0.204)	3
UFP-515	0.48 (0.011)	–	3	0.56 (0.039)		6.43 (0.165)	3
UFP-501	0.13 (0.031)	8.41 (0.071)	3	N.M.	0.060 (0.021)	<=6	3
TIC	0.13 (0.020)	8.37 (0.024)	3	0.09 (0.020)		6.31 (0.345)	3
BNTX	0.36 (0.039)	8.34 (0.135)	3	0.24 (0.040)		8.24 (0.157)	3

enhanced FRC in the MOP receptor, although at greater concentrations and with no measurable plateau (Fig. 1, *a* and *b*). The peptides UFP-505 and dMe-UFP-505 show a clear reversal of IA between receptors (neutral antagonist and inverse agonist at the DOP receptor; both partial agonists at the MOP receptor).

On comparing the intrinsic activities of ligands (Table 1) with the level of constitutive coupling in each receptor (Table 1, first row), roughly half of the Dmt-Tic analogues display remarkable reversions of apparent efficacy on moving from the MOP to the DOP receptor. At least 18 peptides displaying varying degrees of partial agonism at the MOP receptor became inverse agonists or antagonists at DOP receptor.

A Dmt-Tic analogue with quasi-neutral efficacy produced a rightward shift in the concentration-response curves of both the agonist and the inverse agonist without affecting IA (Fig. 1*c*). This pattern is typical of competitive interaction. Similar competitive behavior was observed against ICI-174,864 or the full agonist, DADLE (data not shown). This indicates that the Dmt-Tic analogues and the pentapeptides occupy the same "orthologous" binding site of the receptor.

Conservation of Intrinsic Activities in DOP and MOP Receptors—In contrast to the apparent reversal discussed above, we reached a different conclusion when ligand intrinsic activities were compared directly regardless of the level of each constitutive receptor coupling. Considered above the GDP baseline, the values of ligand IA tend to be similar in both receptors (Table 1). This correspondence was evident when we plotted (Fig. 1*d*) the relationship between ligand IA in the DOP and MOP receptors (only 24 of the 35 ligands could be examined in this graph, because the E_{max} values of several low potency analogues at MOP receptors could not be determined). Ten analogues (Fig. 1*d*, *gray circles*) show IA values that are not statistically different in the two receptors; but even when significant, the differences are relatively small. The global data correlation in Fig. 1*d* is highly significant (0.88, $p < 0.001$) and suggests a general trend: every ligand seems to approach the same level of receptor-G protein coupling on binding MOP or DOP, despite the large difference the receptors show in the empty state.

This phenomenon is not the result of a particular level of receptor expression or G protein composition determined by the engineering of neuroblastoma cells. We used membranes from HEK-293 cell lines (22), where DOP and MOP receptors are present at a ~2.5-fold greater level of expression, to compare the maximal effects of 27 Dmt-Tic peptides (all tested at 10 μM). Despite a slightly larger level of constitutive coupling in both DOP and MOP, consistent with the enhanced expression, this characteristic pattern consisting of equal intrinsic activity with unequal constitutive activity was very similar in the two cell lines (data not shown).

Thus, the G protein coupling responses of empty and ligand-bound opioid receptors delivered conflicting information about ligand efficacy. If considered as the relative change from the receptors base lines, most ligands undergo a reversal of efficacy on passing from one receptor to the other. But if considered as absolute changes, most ligands maintain equal efficacy in the two receptors.

Effects of Ligands on Receptor-Arrestin Coupling—We wondered whether Dmt-Tic ligands would show inverse agonism and/or biased agonism at receptor-arrestin interaction. Using a previously described BRET assay in intact cells (22), we compared the β-arrestin 2 coupling activities of Dmt-Tic analogues in both receptors. All ligands were first screened (data not shown) at saturating concentrations (10 μM). Those producing a detectable change of BRET ratio were further analyzed using concentration-response relationships. One-third of the Dmt-Tic analogues had measurable effects on arrestin coupling in both receptors, but in MOP only three were potent enough to allow concentration-response analysis. E_{max} and pEC_{50} values are listed in Table 2, and curves are shown in Fig. 2, *a* and *b*. Although the basal BRET signal was slightly greater in DOP- than in MOP-expressing cells, no ligand-mediated inhibition was detected, suggesting that such a difference could not be attributed to divergences of constitutive arrestin coupling. Thus, neither DOP nor MOP receptors displayed measurable levels of constitutive activation in recruiting arrestin.

The comparison of arrestin and G protein IA in the DOP receptor shows that agonists display consistently lower efficacy at the former interaction. The extent of such a discrepancy is inversely related to the level of IA (Fig. 2*c*). We reported the same trend previously, using a wider range of different opioid ligand structures (22); it suggests that the strength of receptor

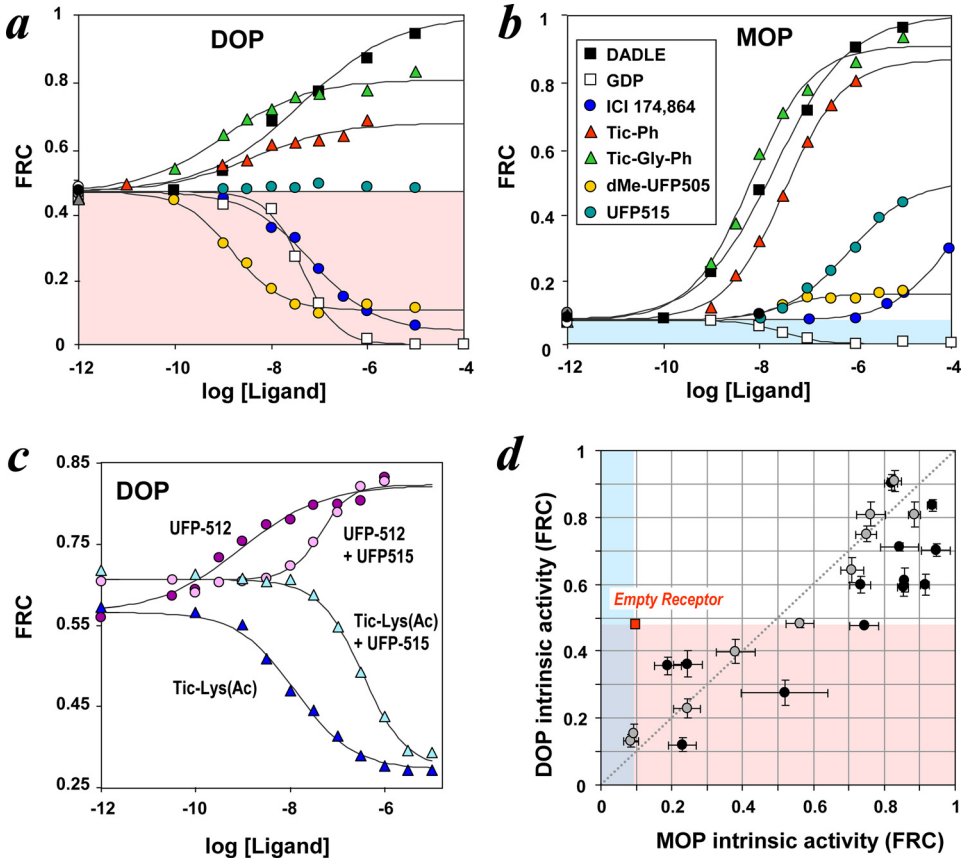

FIGURE 1. **Effect of ligands on opioid receptor-G protein coupling.** *a* and *b*, concentration-dependent increase of FRC (see "Experimental Procedures") in DOP and MOP receptors by the indicated ligands. The level of constitutive coupling in the two systems is shaded. Data are representative of three independent experiments (means of fitted parameters in Table 1). *c*, agonist (UFP-512) and inverse agonist (Tic-Lys(Ac) curves in the absence or presence of the neutral antagonist UFP-515 (50 nM) in DOP receptor. The experiment was repeated twice with comparable results. *d*, intrinsic activities of ligands (as FRC units) in DOP (*y* axis) and MOP receptor (*x* axis). The *gray symbols* indicate values that are not statistically different in the two receptors ($p \geq 0.05$, *t* test). The correlation coefficient among all data is 0.88 ($p < 0.001$).

TABLE 2

Maximal effects (E_{max}) and potency (pEC_{50}) of Dmt-Tic ligands for receptor-arrestin 2 coupling in intact cells

Exp. E_{max} is the effect of the ligand measured at 10 μM.

Ligand	DOP/βARR2		
	Emax (±S.E.)	pEC_{50} (±S.E.)	n
DADLE	1.00 (0.015)	7.41 (0.786)	12
Tic-Glu	0.25 (0.007)	6.70 (0.158)	12
Tic-DGlu	0.02 (0.002)	6.62 (0.204)	3
Bid-Bzl	0.04 (0.007)	6.54 (0.092)	3
UFP-512	0.63 (0.037)	7.68 (0.139)	3
UFP-502	0.70 (0.026)	7.43 (0.059)	4
dMe-UFP-502	0.10 (0.006)	7.43 (0.045)	3
C1-Bid	0.03 (0.005)	7.03 (0.145)	3
Tib	0.07 (0.007)	7.26 (0.161)	3
Tic-Ph	0.04 (0.004)	7.23 (0.251)	3
Tic-Gly-Ph	0.22 (0.013)	7.74 (0.105)	4

Ligand	MOP/βARR2			
	Emax (±S.E.)	Exp. Emax (±S.E.)	pEC_{50} (±S.E.)	n
DADLE	1.00 (0.027)		6.18 (0.148)	8
Bid-Bzl	N.M.	0.03 (0.002)	<=6	2
Bid-Propen	0.06 (0.021)		6.44 (0.071)	3
Bid-cPropyl	N.M.	0.06 (0.003)	<=6	2
UFP-502	N.M.	0.07 (0.007)	<=6	2
Gly-Bid	N.M.	0.04 (0.006)	<=6	2
Tib	N.M.	0.30 (0.063)	<=6	2
Tic-Ph	N.M.	0.50 (0.028)	<=6	2
Tic-Gly-Ph	0.57 (0.042)		6.96 (0.042)	3
UFP-505	0.45 (0.039)		6.54 (0.169)	3

interaction is far lower for arrestin than for G proteins. None of the inverse agonists for G protein exhibited any detectable agonism for arrestin.

Ligand Structural Changes Associated with Modifications of Efficacy—Structure-activity analysis of the data in Table 1 uncovered two modifications of the Dmt-Tic scaffold that are related to loss of efficacy and inverse agonism for DOP receptors.

One is the position of the carboxylic group in the "tripeptide" series of Tic-Dmt analogues. A common motif in this class of ligands is the presence of different amino acids extending the C terminus of the Tic residue (Table 1 and Fig. 3*a*). The replacement of Glu-NH_2 with Gln-COOH (*i.e.* the transfer of the carboxylate anion from the side chain to the peptide backbone) results in a dramatic reduction of IA, which converts a strong partial agonist into an inverse agonist. A similar reduction is observed in the pair of peptides that are extended with the corresponding D-amino acids. Likewise, a corresponding pattern (neutral antagonist becoming inverse agonist) occurs on replacing Asp-NH_2 with Asn-OH (Fig. 3*a*). Thus, the location of the C-terminal carboxylate plays a fundamental role in the efficacy of the ligands for the DOP receptor. Because the IA of such ligands could not be measured in MOP receptors, a comparative assessment of the effect of this modification could not be made.

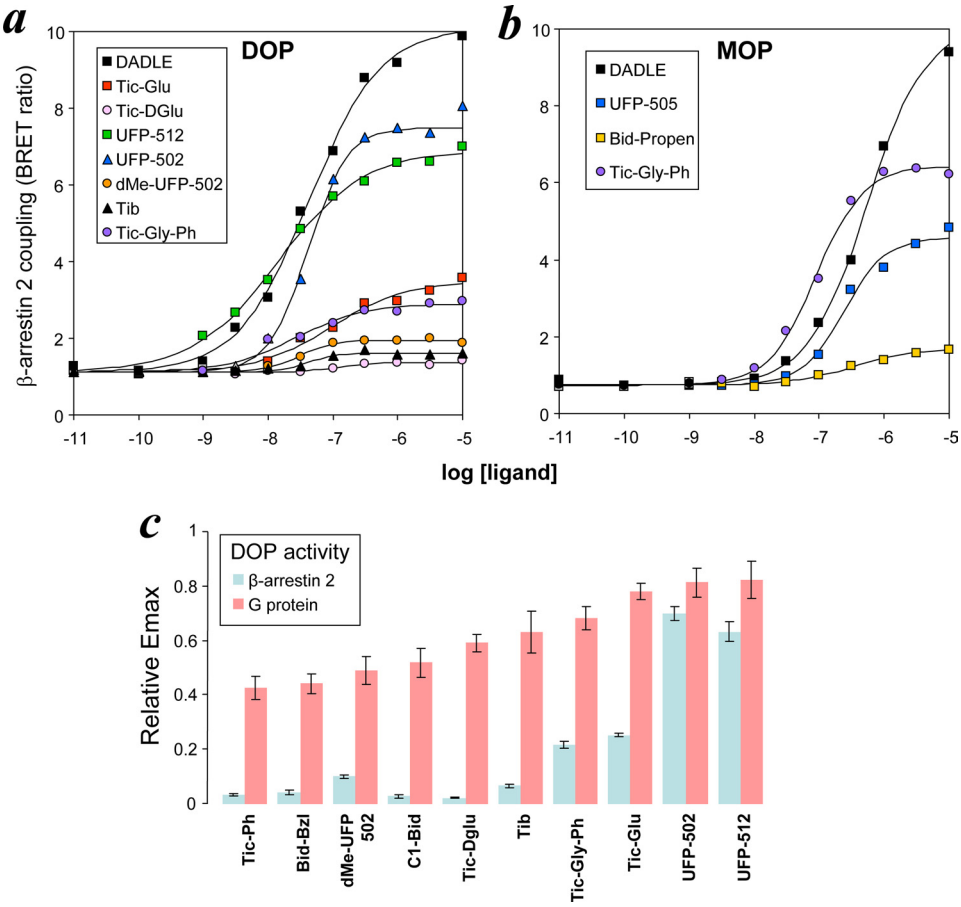

FIGURE 2. **Effect of ligands on opioid receptor-β-arrestin 2 coupling.** *a* and *b*, concentration-response curves for ligand effects on BRET ratio in DOP (*a*) and MOP (*b*) receptors. The means of fitted parameters from three independent experiments are reported in Table 2. *c*, the relative E_{max} values measured in G protein and β-arrestin 2 coupling are compared.

The second modification is the dimethylation of the Dmt amino group. Six pairs of ligands consisting of amino-free and dimethylated versions of the same molecules allowed full concentration-response curve analysis and thus a comparison across receptors. Alkylation reduced IA in both receptors. However, given the difference in spontaneous coupling, this decrease generated inverse agonism in DOP but only reduced the extent of agonism in the MOP receptor (Table 1).

To analyze this effect, we plotted DOP *versus* MOP ligand IA values (Fig. 3*b*). In this graph, the vectors tracing the distance in activity between unsubstituted and substituted analogues measure the joint variation of IA caused by ligand modification in both systems. They have different lengths, because dimethylation has a different effect on each peptide, but the slopes are similar and roughly parallel to the line of perfect correlation. This means that both the direction and magnitude of the loss of IA caused by *N*-methylation are well conserved in DOP and MOP. Therefore, the modification produces an identical reduction of efficacy (presumably acting through an identical mechanism) in both. Yet, if we evaluate the variation with respect to the level of constitutive coupling, the same loss of efficacy converts agonists into inverse agonists at the DOP receptor but only reduces agonism at the MOP receptor.

The effect of methylation on the pEC_{50} of the ligands was instead divergent in the two receptors. The alkylation increased potency in five of six ligands at the DOP receptor but produced either reductions or enhancements of pEC_{50} at the MOP receptors (Fig. 3*c*). These data are consistent with the previous findings that *N*-alkylation of the Dmt-Tic pharmacophore increases the binding affinity for the DOP receptor (25).

The Relationship between Maximal Coupling and the Shift of GDP Apparent Affinity—We used a more precise approach to assess ligand efficacy at MOP and DOP receptors. There is negative cooperativity between ligand and GDP in GPCR systems. Thus, efficacy can be deduced from the effect that the ligand exerts on the apparent inhibition constant (K_i) of GDP.

Fig. 4, *a* and *b* shows typical concentration-response curves for GDP-mediated inhibition of receptor-G protein coupling, obtained in the absence and at saturating concentrations of ligands. The K_i values of GDP become larger as ligand IA increases. Agonists producing the highest level of G protein coupling also raise the inhibition plateau of GDP, as expected for an allosteric interaction. These experiments also allowed us to measure the shift in GDP K_i induced by DOP and MOP receptors in the absence of ligand. Consistent with the difference in constitutive coupling between receptors, the GDP K_i was larger in DOP than in MOP (Fig. 4*c*).

Using ligands covering the full range of efficacy, we examined the relationship between the ligand IA and apparent K_i of GDP (plotted as negative log pK_i) in both receptors. These curves are very similar in DOP and MOP (Fig. 4*d*). In the low ligand IA

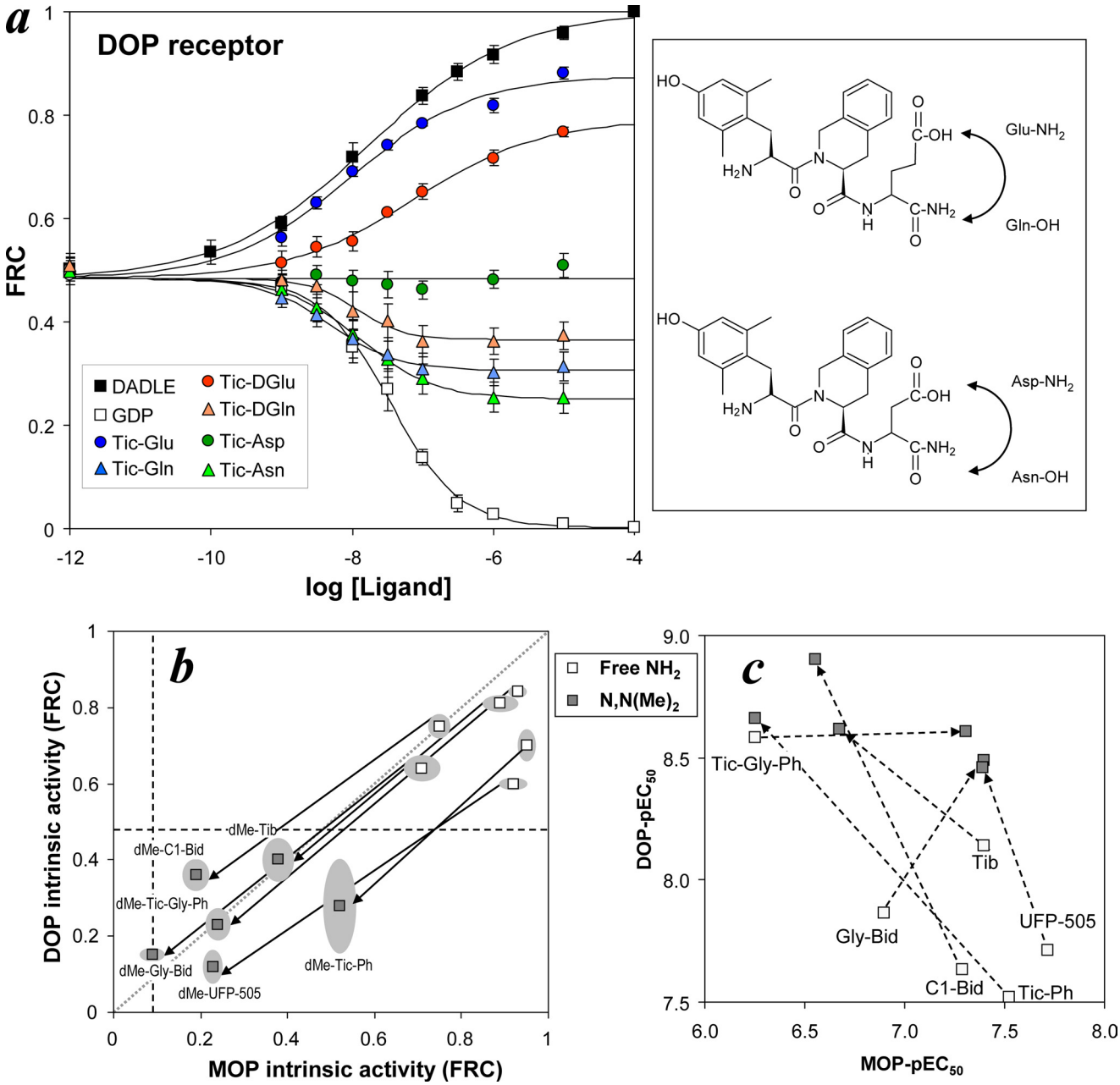

FIGURE 3. **Modifications of Dmt-Tic ligands that generate inverse agonism in DOP.** *a*, concentration-response curves of ligands with C-terminal Glu/Gln or Asp/Asn residues (see *boxed legend*) in DOP receptor (means of three experiments ± S.E.). The *schematic* on the *right* illustrates the shift in position of the free carboxyl group in such ligands. *b*, intrinsic activity of amino-free and *N*,*N*′-dimethylated peptides in MOP and DOP receptors. Data plotted as described for Fig.*1d* are means of three experiments; the *shaded ellipsoids* were drawn around the S.E. in both axes. The *arrows* mark the loss of intrinsic activity in the two receptors. *c*, pEC_{50} (negative log of EC_{50}) values of the same ligands as in *b* are plotted with *arrows* indicating the change in potency.

range, large differences in coupling correspond to minimal changes of pK_i and vice versa in the high range (Fig. 4*d*). This curvilinear shape is due to the dual components of the free energy change that underlies K_i. One, related to the binding interaction, is constant. The other, reflecting cooperativity, varies with ligand efficacy. Thus, at lower ligand IA values (small cooperative effects), changes in K_i barely exceed the experimental error, but at greater values the differences become increasingly visible. Note that the changes in GDP pK_i caused by empty receptors are well aligned with those induced by ligands, indicating that the level of coupling in the unbound receptor is predictable from those observed in ligand-bound receptors.

For a system consisting of two ligands interacting at different sites of the same protein complex, the shift in the apparent affinity of one ligand caused by saturating concentrations of the second provides a direct measure of the free energy coupling existing between the two binding processes (16). We computed such coupling constants (*i.e.* net differences in GDP pK_i between the absence and presence of ligand) for peptides with the same IA in both receptors. Plotting such values in the MOP *versus* DOP receptor yields a linear relationship with unit slope

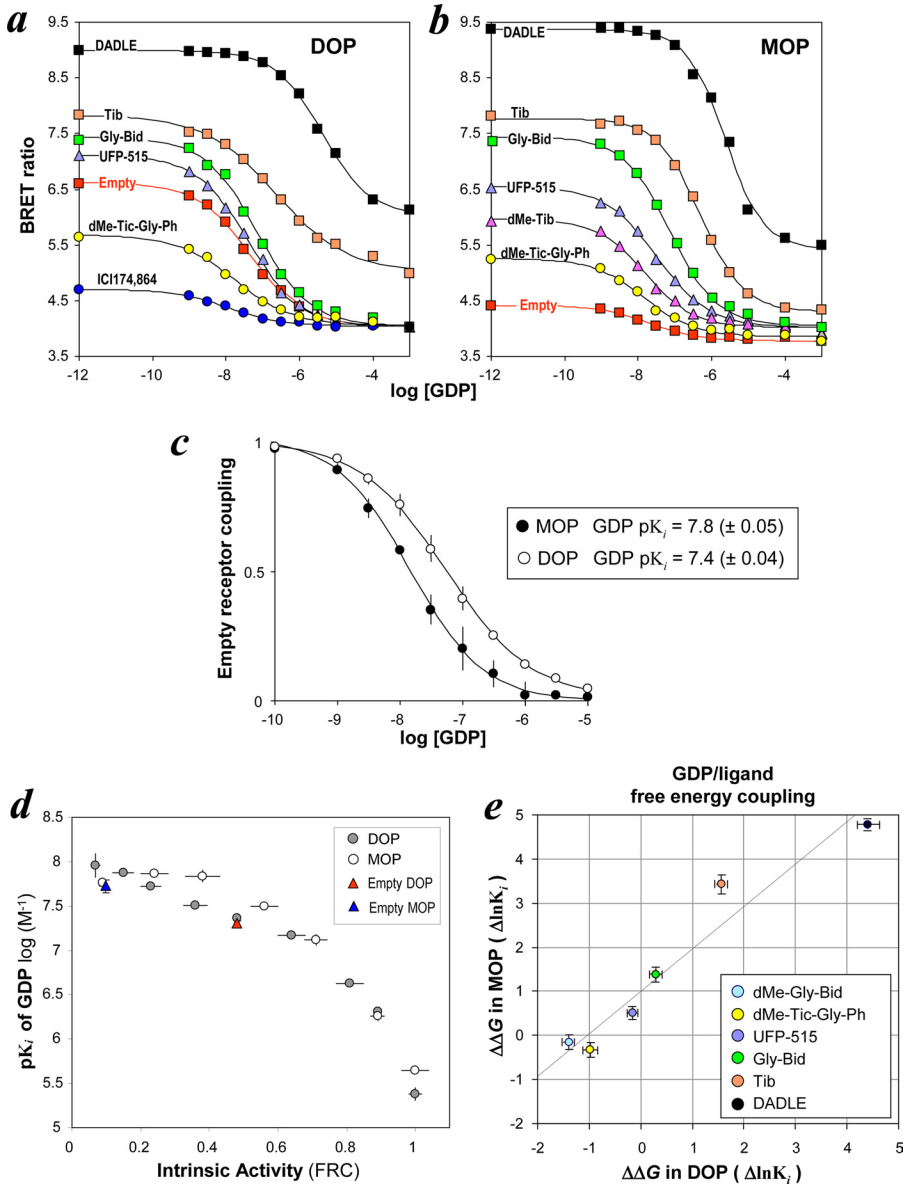

FIGURE 4. **Effect of ligands on apparent GDP affinity.** *a* and *b*, concentration-response curves for GDP-mediated inhibition of DOP and MOP receptor coupling induced by the indicated ligands (10 μM). The *y* axis data are the measured BRET ratios. *c*, GDP inhibition of DOP and MOP constitutive coupling. Curves were averaged ± S.E. from 15 experiments after normalizing the data as a fraction of the net effect in the absence of nucleotide. The difference in K_i values is significant (analysis of variance, $F = 40.2$, $p < 1 \times 10^{-6}$). *d*, the negative log of K_i (pK_i) in DOP and MOP computed from GDP curves (as shown in *a* and *b*) are plotted as a function of the ligand-intrinsic activities (Table 1). Data are means ± S.E. from three experiments. *e*, free energy coupling values ($\Delta\Delta G$ in *RT* units) for the negative cooperativity between ligands and GDP in DOP and MOP, calculated from the difference in the natural logarithms of GDP K_i between the absence and presence of ligand. Data point are means ± S.E. of three experiments. Linear regression (*solid line*) yields slope 0.96 ± 0.11 and intercept 0.99 ± 0.22.

and nonzero intercept (Fig. 4*e*). The unit slope indicates that for any given change of ligand structure there are identical changes of allosteric coupling (efficacy) in the two receptor-G protein systems. But the upward shift of the line on the *y* axis indicates that all free energy coupling values in the DOP receptor are uniformly reduced by a constant factor compared with the MOP receptor. The size of this shift (≈1 unit of free energy on the *RT* scale) is equivalent to the difference in GDP K_i between the two empty receptors (Fig. 4*c*).

Model of Constitutive Activation—The overall pattern of constitutive activation and inverse agonism documented in this study is in contrast to the prediction of models such as the ternary complex model (TCM) (14) and/or the extended (5, 15) or cubic (17) ternary complex models.

Assuming that DOP and MOP differ only in constitutive coupling and that Dmt-Tic with equal IA have identical molecular efficacies, we computed how that pattern should be predicted according to the TCM (Fig. 5*a* and Equation 1 under "Appendix"). This "TCM fitting" analysis shows that a difference in constitutive activity (*i.e.* $M'_{DOP} > M'_{MOP}$) cannot coexist with equal levels of maximal activity, if the molecular efficacies of the ligands are identical in the two receptors (*i.e.* $\alpha'_{iDOP} = \alpha'_{iMOP}$). Moreover a change in constitutive activation cannot alter the rank of ligand-intrinsic activities, *e.g.* inverse agonists inhibit spontane-

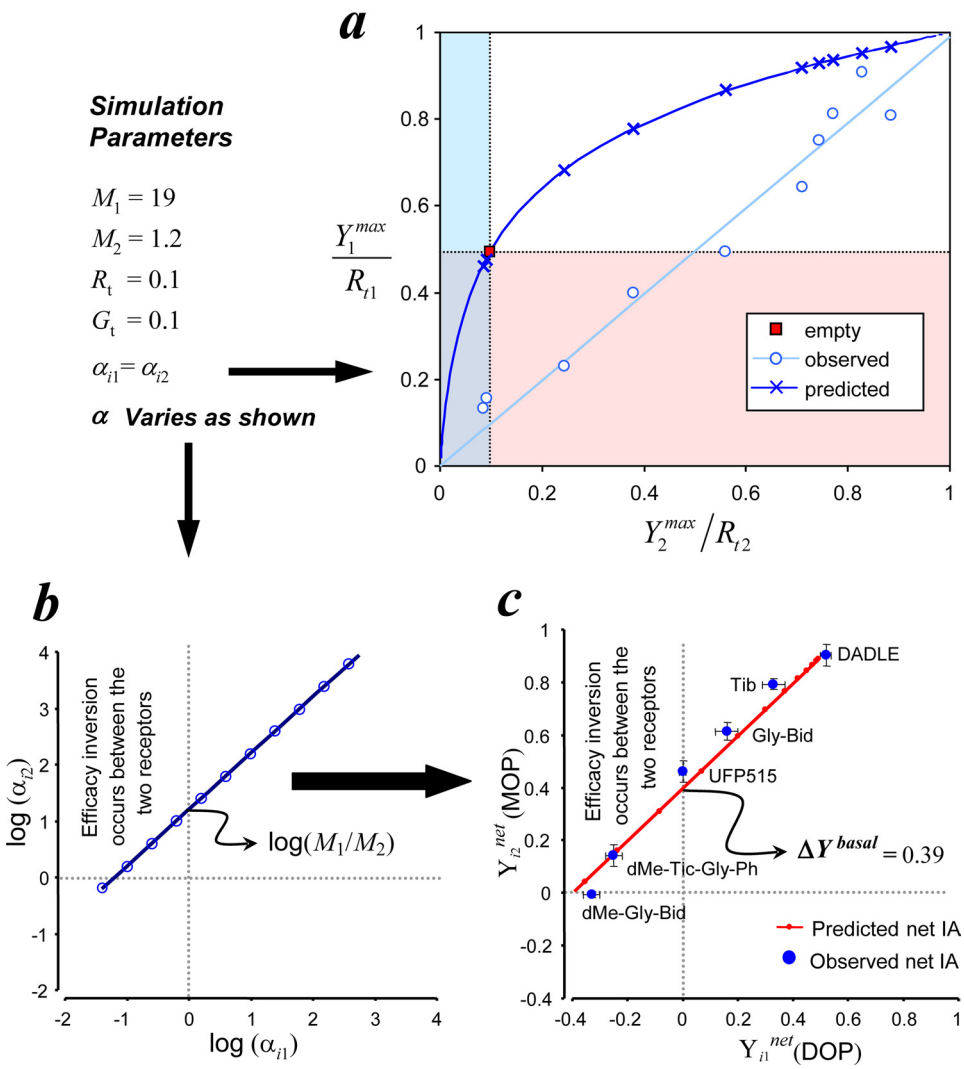

FIGURE 5. **Relationship between ligand IA in DOP and MOP, showing a comparison of the experimental observations and TCM predictions.** *a*, simulated IA data represent Y^{max} values calculated (with the TCM parameter values indicated) using Equation 1 (see "Appendix") for ligands sharing equal α values (ranging from 0.01 to 1000) at two receptors (R_1 and R_2) that have different *M* values. Y^{max} is normalized with respect to total receptor concentration. The theoretical data (—) are shown with the experimental data replotted from Fig. 1 (○; only ligand IA with nonstatistically different MOP and DOP values is shown). ×, projections of experimental data onto the predicted curve; ■, level of constitutive coupling (empty receptor). The *shaded areas* indicate the range of inverse agonism (*i.e.* where ligands with $\alpha' < 1$ are expected to inhibit spontaneous coupling). *b*, a set of log α values chosen according to Equation 2 (see "Appendix") for the two receptors. Values of M_1 and M_2 are shown. *c*, calculated net responses induced by the ligands that are identified with the α values shown in *b*. The net response is given as the difference between total concentrations of *RG* complexes (*i.e. RG* + *HRG*) calculated in the absence or presence of saturating ligand. The calculated response is normalized as described for *b*. Experimental net responses (●) for the ligands are calculated from *a*.

ous association in both the highly constitutively active and slightly constitutively active receptor, even if in the latter it might be difficult to quantify the effect (see "Appendix" and Fig. 5*a*).

The same analysis indicates that to observe equal IA values the molecular efficacy of the ligands for DOP should be reduced uniformly by a quota of free energy that is exactly equivalent to the difference in G protein binding affinity between DOP and MOP receptors (Fig. 5, *b* and *c*, and under "Appendix"). Thus, both the theoretical analysis (Fig. 5) and the experimental measurement of GDP cooperativity (Fig 4*e*) converge to an identical conclusion: the apparent efficacies of ligands in the constitutively active receptor are uniformly changed by the process of constitutive activation.

We developed a different extension of the TCM model, capable of explaining the phenomenology reported in this study (see "Appendix"). In former models, constitutive activity depends on the equilibrium between the active and inactive forms of the receptor. This equilibrium is cooperatively linked to ligand binding in the same way as it is to the association between the receptor and G protein. Thus, for any change in magnitude of that equilibrium, constitutive and ligand-induced complexes are invariantly ordered on the coupling scale (15). In the present model, however, the allosteric transition is conceived as a change in energy state of the system, which may occur in either or both of the reacting proteins. This change represents the energy cost of the transition from spontaneously occurring to ligand-controlled multiprotein complexes and is linked by strong negative cooperativity to every ligand binding process. Ligands must restrain spontaneous coupling to drive the system to the associated ligand-bound form. Thus constitutive and ligand-driven coupling are competitive nonconverging paths that lead to activation of the system (see "Appendix").

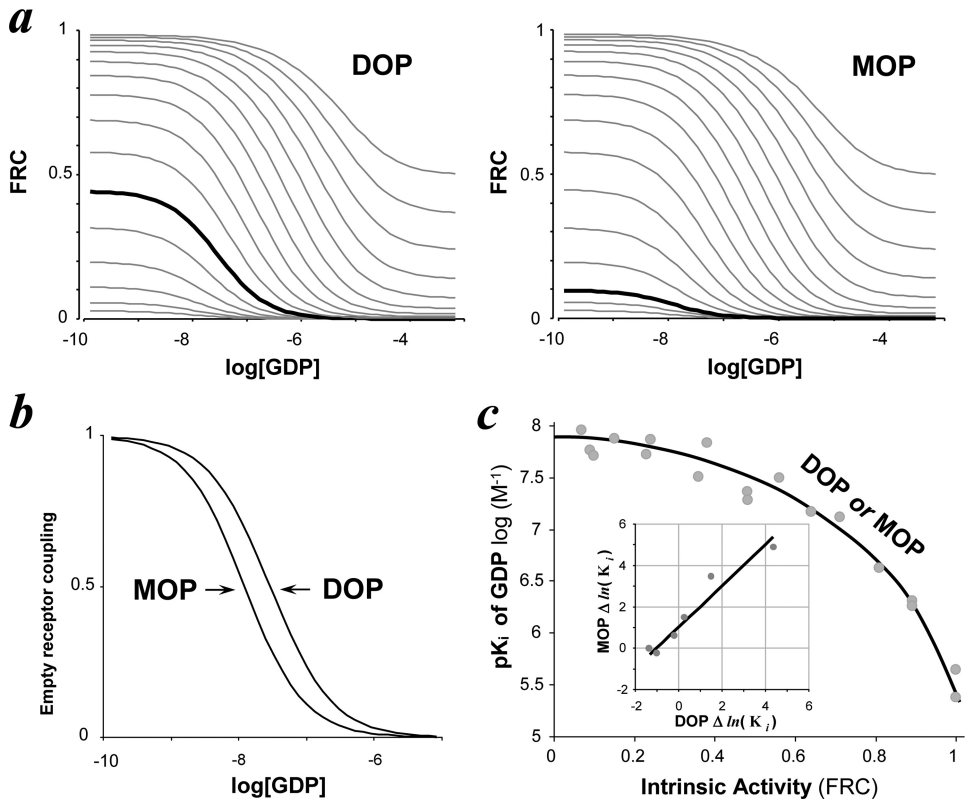

FIGURE 6. **Results of simulations made according to the allosteric model illustrated in Fig. 8 and under "Appendix."** Two systems with high and low levels of spontaneous activity (called DOP and MOP, respectively) were simulated. FRC is the sum of constitutive and ligand-bound coupled species ([*RG*] + [*HRG*])/[R_{total}]). The two systems differ only in the coupling factor, γ ($\gamma = 280$ in DOP and 5 in MOP). All other parameter values are equal in DOP and MOP: $R_{total} = G_{total} = 10^{-10}$; $M = 10^{9}$; $K = 10^{-5}$; $L = 10^{8}$; $J = 0.05$; $\beta = 10^{-4}$; $\delta = 10^{-3}$; ligand efficacy (α) varies from 0.1 to 14000. *a*, simulated curves for GDP inhibition of FRC induced by the ligands in DOP and MOP. *Thick lines* indicate no ligand (compare with Fig. 4, *a* and *b*). *b*, from such curves we calculated the normalized inhibition of constitutive coupling in DOP and MOP (compare IC_{50} shifts with those in Fig. 4*c*). *c*, the simulated relationship between GDP pK_i and ligand intrinsic activities together with the ligand-GDP coupling $\Delta\Delta G$ values (*inset*) in DOP and MOP. The *solid curves* are simulated data superimposed on the experimental data (*gray dot*) replotted from Fig. 4, *d* and *e*.

The simulations in Figs. 6 and 7 show how the sole enhancement of the equilibrium for this intramolecular transition, without any other change in ligand-dependent parameters, can generate a pattern of constitutive activation that reproduces all of the phenomenology described in this article. Identical results with minor adjustments in parameter values can be generated using all three versions of the model discussed under "Appendix" (data not shown).

To challenge the model, an experiment was first predicted *in silico*. If, on adding a suitable concentration of GDP to the highly constitutive active subtype, we equalized the levels of spontaneous coupling in the two receptors, the correspondence of ligand-intrinsic activities should be lost (Fig. 7*a*). We executed the same experiment in real membranes using a subset of ligands with similar intrinsic activities (Fig. 7*b*). Simultaneous fitting of the concentration-response curves obtained in parallel MOP and DOP membrane assays confirmed that the ligands share indistinguishable IA values in the receptors; but this symmetry was disrupted upon the addition of 200 nM GDP to DOP, which lowered its constitutive activity to a level closer to that of MOP (Fig. 7*b*). Consequently, the linear relationship between ligand IA in the two receptors is converted to a hyperbolic relationship (Fig. 7*c*).

DISCUSSION

In this study we have compared the activity of a congeneric series of ligands for wild-type DOP and MOP receptors using a BRET-based measurement of receptor-G protein interaction in membranes. As with GTPγS binding, this assay provides a signal that is directly related to receptor-G protein association but brings two additional advantages. The ability to assess both receptor-G protein association and the apparent affinity of nucleotides, and the capacity to measure receptor-G protein coupling of both ligand-bound and unbound receptor. With tagged proteins expressed at similar levels, BRET allows the comparison of constitutive and ligand-induced activities across different receptors on the same scale.

We have reported here several new findings on the constitutive activation and inverse agonism of the DOP receptor. First, we found a major difference in the extent of constitutive activation between the DOP and MOP receptors. Spontaneous G protein coupling is 4–5 times greater in the DOP than in the MOP receptor. Indeed, the wild-type DOP receptor appears as a natural, constitutively active mutant of the MOP receptor.

Second, we identified 16 ligand structures that act as DOP inverse agonists and display a remarkable variation in the extent of apparent negative efficacy. This effect is mediated by occupation of the same binding site of enkephalins and other opioid ligands, as indicated by competition with a pure antagonist. Thus, inverse agonism is a frequent event in ligands based on the Dmt-Tic scaffold, making this pharma-

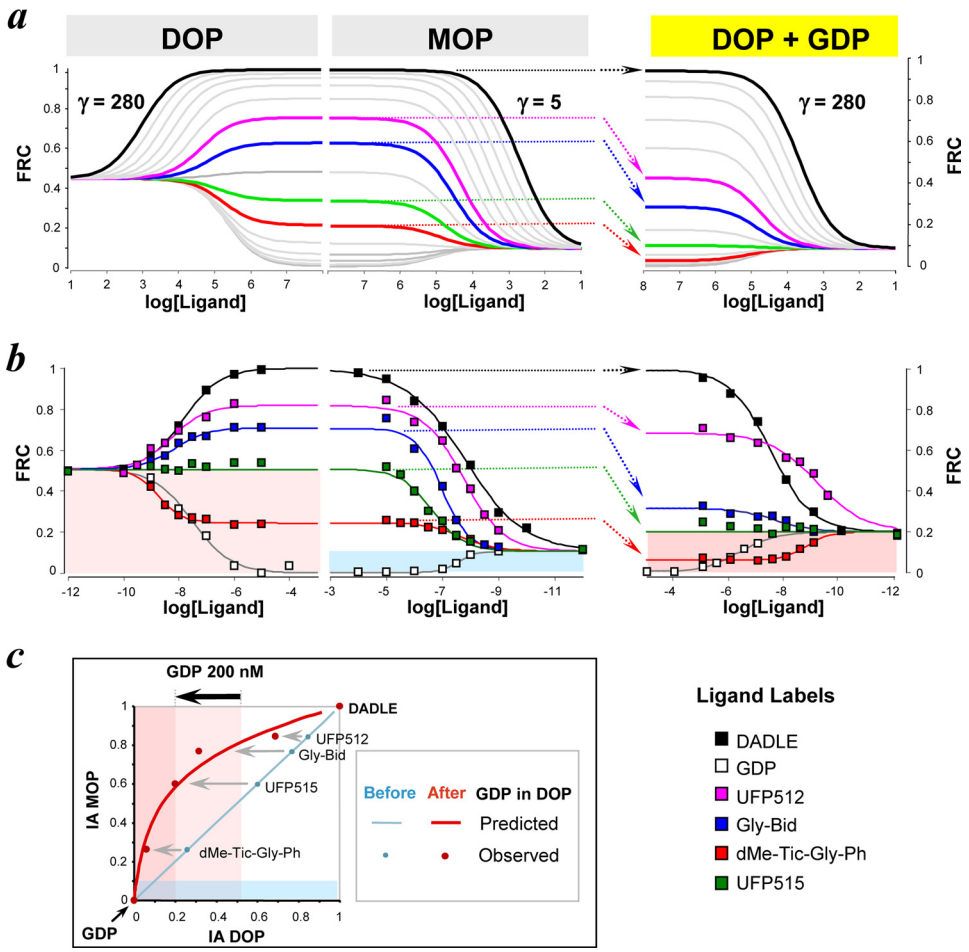

FIGURE 7. **GDP breaks the correspondence of ligand intrinsic activity between DOP and MOP receptors.** *a*, results of simulations made according to the models presented in Fig. 8. Simulated FRC and parameter values are like those in Fig. 6. An increase of γ (as shown) is used to generate enhanced basal coupling in DOP (the *x* axes of the *second* and *third panels* are ordered in opposite directions to facilitate E_{max} comparison across the panels). The *third panel* shows DOP as does the *first panel* but simulated in the presence of ligand *N* at a concentration sufficient to lower basal coupling to the same level as MOP. Note the break in *E*max symmetry. *b*, *curves* obtained in DOP and MOP receptor membranes for the indicated ligands (without GDP) were globally fitted (*first two panels*). Sharing the same E_{max} for each ligand in DOP and MOP did not change significantly ($p = 0.23$) the goodness of fit according to the extra sum of square principle (29) The *third panel* shows the same ligands assayed in DOP with 200 nM GDP (which lowers the basal activity of DOP close to that of MOP). The *shaded areas* show basal couplings; concentration axes are ordered as in *a*. The experiments were repeated twice with identical results. *c*, observed and predicted E_{max} values in DOP and MOP with or without GDP, as indicated. The predicted and observed values are taken from *a* and *b*, respectively. Note the quantitative agreement between experimental observations and predictions.

cophore the ideal structural template for investigations of negative efficacy. No ligand exhibited inverse agonism at receptor-arrestin interaction, suggesting that the difference in constitutive activation between MOP and DOP is restricted to receptor-G protein interactions.

Third, we identified two main structural modifications of the Dmt-Tic scaffold that are correlated with the occurrence of inverse agonism in the ligands. These modifications engage opposite ends of the molecule and involve groups with opposite charge. The position of the anionic carboxylate at the C terminus and the dimethylation of the N-terminal cationic amine conferred the strongest level of inverse agonism observed for Dmt-Tic ligands in this work. This suggests that electrostatic interactions in the receptor binding pocket play a major role in determining inverse agonism. Perhaps the relatively constrained structure of the Dmt-Tic template optimizes the orientation of charged groups, which likely interact with polar residues on different domains of the receptor's transmembrane bundle. Analysis of Dmt-Tic-bound receptor crystals should provide valuable information on the nature of such structural requirements.

However, the most important finding in this study is a surprising new feature of receptor constitutive activation. Ligands that move the level of receptor-G protein coupling into opposite directions from the ligand-free receptor base line of DOP and MOP (thus apparently showing opposite efficacy in the two receptors) generate the same level of G protein coupling in both systems, thus exhibiting identical IA in the two receptors. Therefore, inverse agonists in the highly constitutively coupled DOP receptor appear as agonists for the slightly constitutively coupled MOP receptor.

One possible explanation is that the correspondence of intrinsic activity in the two receptors is fortuitous. Despite the remarkable similarity shown in atomic resolution structures (30, 31), MOP and DOP receptors are different proteins. Thus, ligands can have opposite efficacy in the two receptors, and yet

by chance, some might converge to similar levels of "absolute" coupling.

Several indications make this explanation inconsistent with experimental evidence. One is probability. Nearly half of the ligands showed statistically indistinguishable IA values at MOP and DOP, and the global correlation among all values was highly significant. Thus, the odds in favor of a randomly generated equivalence of intrinsic activities are extremely low. In addition, two mechanistic arguments point to the same conclusion: the identical loss of IA that *N*-alkylation of the ligands causes in the two receptors and the overlapping relationships between changes in GDP affinity and ligands effects. Both arguments support the notion that ligand efficacy and IA are strictly related. Thus, Dmt-Tic analogues have identical or very similar efficacies at DOP and MOP receptors, despite the divergent direction in which G protein association is changed from the level of spontaneous coupling in each receptor.

Our data seem to suggest that ligand-induced and constitutive receptor activation result from different mechanisms. However, there is quantitative agreement between the effects of empty and ligand-bound receptors on GDP affinity. One clue comes from the study of the ligand/GDP free energy coupling values in the two receptors (Fig. 4*e*). This analysis shows that ligands with equal IA in MOP and DOP display an equal diminution of allosteric effect in the constitutively active DOP. Measured as free energy units, this constant loss is identical to the shift of GDP affinity that the two receptors show in the unbound state. This suggests that the mechanism causing constitutive activation in the DOP receptor can also collectively reduce the allosteric effects of all ligands, regardless of their molecular efficacy. Put simply, constitutive activation can cut a common energy cost that all ligands pay when driving receptors to the G protein-associated form.

Based on the above analysis, we developed a new extension of the TCM model (see under "Appendix"), which is capable of explaining the phenomenology reported in this study. Two interesting mechanistic implications can be drawn from this modeling analysis.

The first is the nature of linkage between ligand-dependent and independent activation. Unlike the concerted shift toward a common allosteric conformation of previous models, this alternative view predicts that all ligands exert negative cooperativity against the process of constitutive activation. Therefore, no ligand-bound state of the system can be energetically equivalent to the ligand-free state. This agrees with a recent single molecule force spectroscopy study of β_2-adrenoceptors bound to ligands of differing efficacies in which it is shown that no ligand-bound receptor form can exactly match the energetic, kinetic, and mechanical pattern of the empty receptor (32).

The second is the dual allosteric process underlying molecular efficacy. There is a ligand-specific cooperative effect that stabilizes the receptor-transducer complex (α) but also a shared anticooperative "binding effect" (β) that every ligand exerts in raising the free energy barrier for spontaneous coupling. This adds to and may cancel the free energy change of the first. Therefore, a ligand with unchanged ability to stabilize the receptor-transducer complex can show agonism in a slightly intrinsically coupled receptor but inverse agonism when a reduction of the energy barrier generates constitutive coupling. It follows that the direction in which ligands steer basal receptor activity is not a reliable indicator of molecular efficacy.

We do not know how prevalent the mechanism of inverse agonism observed here might be among GPCRs. Of the two additional types of inverse agonists that we tested (Table 1), the naltrexone derivative BNTX displayed close IA values in the two receptors, with the blend of DOP inverse agonism and MOP partial agonism that is typical of Dmt-Tic peptides. But the pentapeptide ICI-174864, even if the E_{max} value at MOP was not measurable, clearly showed a different trend, suggesting a true reversal of molecular efficacy in the two receptors. Thus, it is possible that the phenomenon described in this article depends on the particular way in which certain structural classes of ligands interact with the binding pocket. Obviously, further studies on additional congeneric series of ligands in several GPCRs will be required. However, the anticooperativity that opposes ligand-induced to spontaneous coupling, which the behavior of Dmt-Tic ligands unveils, likely depicts a general feature of GPCRs and may bring more insight into the functional chemistry of these molecules.

APPENDIX

Agonism and Inverse Agonism in the Ternary Complex Model—The TCM depicts the interactions among ligand (*H*), receptor (*R*), and G protein (*G*) (Fig. 8) with three independent parameters: two affinity constants, K' and M', govern the formation of the *HR* and *RG* complexes in the absence of G or H, whereas an allosteric constant, α', describes the thermodynamic coupling between *H* and *G* binding to *R* (the prime symbol stands for effective constants as will be explained later). For each receptor-G protein system, α' encapsulates the molecular efficacy of ligands, and M' controls constitutive coupling. Consider two receptors (R_1 and R_2) that differ in affinity for a common G protein (*i.e.* $M'_1 > M'_2$) and interact with a set of ligands having equal molecular efficacies in the two receptors (*i.e.* $\alpha'_{i1} = \alpha'_{i2}$). Ligand-intrinsic activities (*i.e.* the asymptotic level of ligand-induced coupling, Y^{max}), is given as

$$Y_{ij}^{max} = \lim_{[H_i]\to\infty} ([R_jG] + [H_iR_jG])$$

$$= \frac{1}{2}\left(R_{t_j} + G_t + \frac{1}{\alpha'_{ij}M_j'} - \sqrt{\left(R_{t_j} + G_t + \frac{1}{\alpha'_{ij}M_j'}\right)^2 - 4R_{t_j}G_t}\right) \quad \text{(Eq. 1)}$$

where *i* and *j* label different ligands and receptors, respectively, and *t* is total reactant concentration.

As shown in Fig. 5*a*, given that $M'_{DOP} > M'_{MOP}$, $R_{t_{DOP}} = R_{t_{MOP}}$, G_t = constant, and $\alpha'_{iDOP} = \alpha'_{iMOP}$, Equation 1 predicts that ligand IA cannot be equal at the two receptors, nor can the increase in M' generate an apparent reversion from positive to inverse agonism. Thus, the TCM cannot explain the pattern of inverse agonism in Dmt-Tic ligands, unless we postulate that a peculiar change in the α' value of each ligand can generate by chance a linear IA relation between the two receptors. Yet Equation 1 also defines which condition is required to observe equal IA ($Y_{i1}^{max} = Y_{i2}^{max}$) with unequal

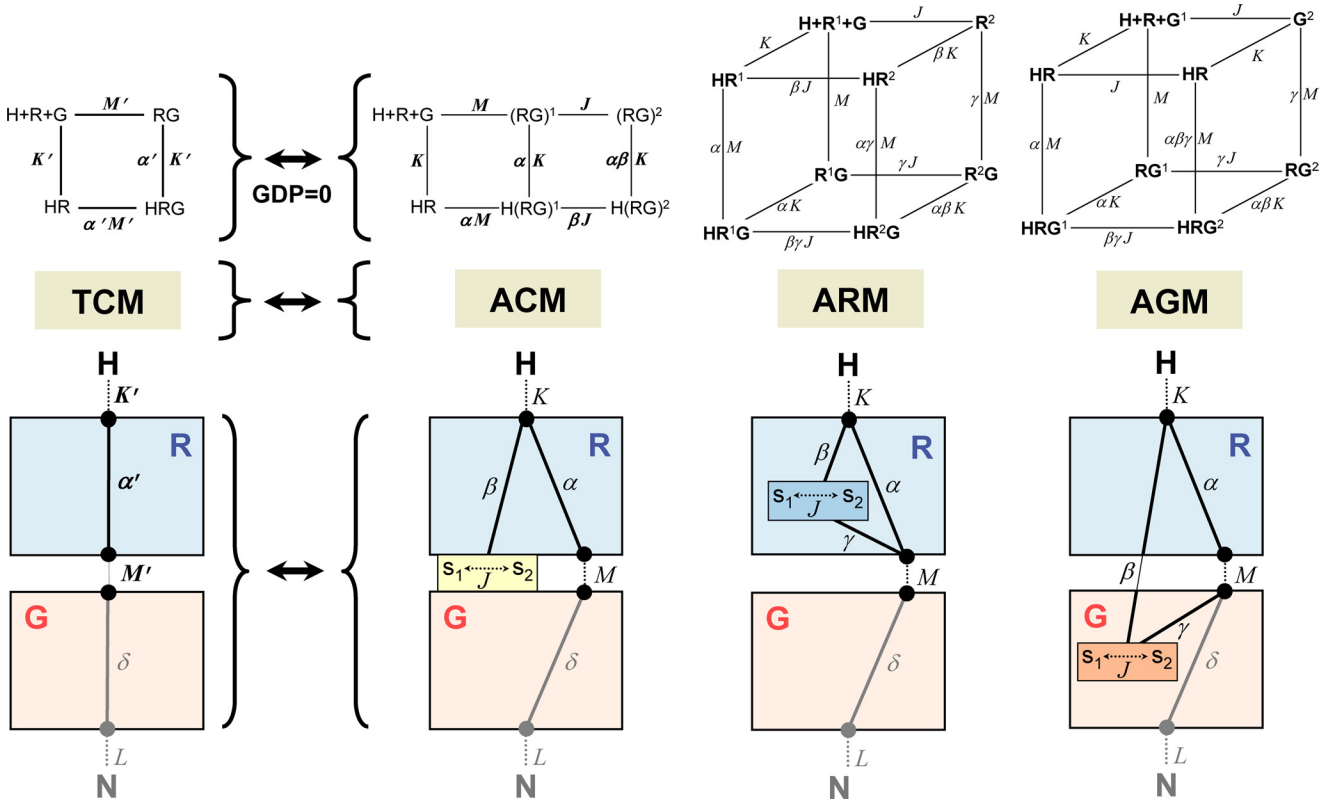

FIGURE 8. **The three allosteric model versions that can equivalently explain the joint variation between *RG* affinity and efficacy.** The original TCM, which such models extend, is shown in the *leftmost column*. *First row*, standard reaction schemes are shown by omitting ligand *N* and related pathways to simplify the drawings. *Second row*, schematic representation of thermodynamic couplings and allosteric equilibria (35). Receptor (*R*) and G protein (*G*) are shown as *shaded boxes*, binding sites as *circles*, binding associations as *dotted lines*, and thermodynamic linkages as *solid lines*. The allosteric transition between the two energy states S_1 and S_2 (*superscripts* in *first row* and *boxed equilibria* in *second row*) is differently located in the three versions: *R-G* interface (in ACM), *R* (in ARM), or *G* (in AGM). In all versions the allosteric equilibrium constant *J* is defined as the ratio $[S_2]/[S_1]$.

constitutive coupling ($M'_1 \neq M'_2$), *i.e.* $\alpha'_{i1}M'_1 = \alpha'_{i2}M'_2$. Written in log form this yields.

$$\log(\alpha'_{i1}) = \log(\alpha'_{i2}) + \log\left(\frac{M'_2}{M'_1}\right) \qquad \text{(Eq. 2)}$$

This means that equal maximal responses in the two receptors ($Y^{max}_{iDOP} = Y^{max}_{iMOP}$) are possible if the allosteric coupling free energy of the ligands (*i.e.* $\log\alpha'_{ij}$) in the highly constitutive active receptor is diminished by a constant amount, which is equal to the free energy difference (*i.e.* $\log[M'_2/M'_1]$) for the formation of the *RG* complex by the two empty receptors (Fig. 5, *b* and *c*). This analysis implies a thermodynamic linkage between *RG* affinity (M') and ligand efficacy (α'), so that a change in the first can uniformly change the second. Such a covariance of M' and α' cannot be defined within the macroscopic framework of the TCM.

Minimal Models That Link Apparent Ligand Efficacy to Constitutive Activity—The three parameters of the TCM must be considered apparent or "effective" constants. Although both K' and M' include an intra- and intermolecular free energy component, they are defined as pure bimolecular associations because the intramolecular contribution is not experimentally measurable (33). Also, the ligand-induced perturbation α' can only be appraised as "additive" free energy of the bimolecular interactions. In this sense the three parameters are independent. If, however, we find covariance between α' and M' (as we do here), it means that the intramolecular perturbation underlying *RG* binding does not simply add to but also interacts with ligand-induced perturbations. In previous work (15) a different covariance between α' and K' was made explicit in the model, assuming an allosteric switch of the receptor between functional states, because the experimental readout in those studies was the signaling activity of receptor mutants.

In this study we measured the assembly of *R*-*G*$\alpha\beta\gamma$ complexes in the absence or presence of ligands or nucleotide. Moreover, the linkage between α' and M' shows up as an equal energy cost that affects all ligand-induced perturbations regardless of their identity. Thus, to make explicit this intrinsic link we postulated an intramolecular change between two different energy states (S_1 and S_2) controlled by a first-order constant, *J*. Because this transition can occur with equal probability in *R*, *G*, or *RG*, we analyzed in parallel all three possible versions of the model, and named them accordingly: ACM (allosteric complex model), ARM (allosteric receptor model), and AGM (allosteric G protein model) (Fig. 8).

The interaction among the two protein species (*R* and *G*), each binding a distinct ligand (peptide *H* and nucleotide *N*), leads to the formation of the coupled forms with and without ligands (*i.e.* the BRET-emitting species) and depends on the *J*-driven state transition ($S_1 \leftrightarrow S_2$) and its cooperative linkage to the binding events. Although all three models describe quite complex reaction schemes, we used two simplifications to analyze how the parameter configurations predict the BRET

response. First, all parameters in the three versions can be reduced by exact functions to the effective parameters, α' and M', of a "macroscopic" TCM equivalent scheme; thus, we could use this approach to define analytically which variations in model parameters would lead to a joint variation of α' and M'. Second, in line with the course of the experiments presented here (conducted in the absence and presence of GDP) we analyzed model behavior first in the absence and next in the presence of ligand *N*, which greatly simplified the task.

Parameter Space in the Absence of GDP—In all three model versions (Fig. 8), the coupling constants β and γ indicate the cooperativity between the state transition ($S_1 \leftrightarrow S_2$) and the binding interactions $H \leftrightarrow R$ and $R \leftrightarrow G$, respectively, whereas α (which gauges ligand efficacy in all versions) is the direct coupling between those binding events. In the absence of *N* (reaction schemes in Fig. 8), the relationship between model parameters and the effective parameters of the equivalent TCM are as follows.

(**ACM**) $$M' = M(1 + J) \quad \alpha' = \alpha\frac{1 + \beta J}{1 + J} \qquad \text{(Eq. 3)}$$

(**ARM**) $$M' = M\frac{(1 + \gamma J)}{1 + J} \quad \alpha' = \alpha\frac{(1 + \beta\gamma J)(1 + J)}{(1 + \beta J)(1 + \gamma J)} \qquad \text{(Eq. 4)}$$

(**AGM**) $$M' = M\frac{(1 + \gamma J)}{1 + J} \quad \alpha' = \alpha\frac{(1 + \beta\gamma J)}{(1 + \gamma J)} \qquad \text{(Eq. 5)}$$

As shown above in Equation 2, the condition to maintain equal ligand IA across receptors is: $\alpha'_{i1}M'_1/\alpha'_{i2}M'_2$. Using Equations 3–5, this constraint can be rewritten in terms of the parameters in the three model versions as

(**ACM**) $$\frac{\alpha_{i1}M_1(1 + \beta_{i1}J_1)}{\alpha_{i2}M_2(1 + \beta_{i2}J_2)} = 1 \qquad \text{(Eq. 6)}$$

(**ARM**) $$\frac{\alpha_{i1}M_1(1 + \beta_{i1}\gamma_1J_1)(1 + \beta_{i2}J_2)}{\alpha_{i2}M_2(1 + \beta_{i2}\gamma_2J_2)(1 + \beta_{i1}J_1)} = 1 \qquad \text{(Eq. 7)}$$

(**AGM**) $$\frac{\alpha_{i1}M_1(1 + \beta_{i1}\gamma_1J)}{\alpha_{i2}M_2(1 + \beta_{i2}\gamma_2J)} = 1 \qquad \text{(Eq. 8)}$$

This can be further simplified by the following points. (*a*) As α does not contribute to M' nor M to α', we can set $\alpha_{i1}/\alpha_{i2} = 1$ and $M_1/M_2 = 1$. (*b*) There is also no contribution of β to M', and thus the change of M' should be caused by a variation in J and/or γ. To change M' significantly, either J (in ACM) or γJ (in ARM or AGM) must be $\gg 1$. (*c*) To satisfy Equations 6–8, β must be small enough to balance the variation in J or γ. Thus, even if β varies across ligands, this variation would have negligible effects on model output (*i.e.* $\beta J \ll 1$ or $\beta\gamma J \ll 1$).

Hence, Equations 6–8 reduce to

(**ACM**) $$\frac{(1 + \beta_{i1}J_1)}{(1 + \beta_{i2}J_2)} = 1 \qquad \text{(Eq. 9)}$$

(**ARM**) $$\frac{(1 + \beta_{i1}\gamma_1J_1)}{(1 + \beta_{i2}\gamma_2J_2)} = 1 \qquad \text{(Eq. 10)}$$

(**AGM**) $$\frac{(1 + \beta_{i1}\gamma_1J)}{(1 + \beta_{i2}\gamma_2J)} = 1 \qquad \text{(Eq. 11)}$$

This final result underscores the symmetry and equivalence of the three versions both in terms of algebraic manipulation and predicted output. Also, the above rules provide guidance for a mechanistic interpretation of the parameters. It is clear from point *b* that J and/or γ looks like the major free energy constraint that limits constitutive coupling in the system. Likewise, the boundaries of the β values (see point *c*) indicate that all receptor ligands regardless of their efficacy (α) must invariably exert a strong negative cooperative effect against the state transition driven by J.

Parameter Space in the Presence of GDP—The presence of guanine nucleotide *N* (which binds to *G* with affinity *L*) does not change the constraints for the parameters discussed above (M, α, J, β, and γ) but introduces an additional coupling constant, δ. This describes the cooperative interaction between the binding of *R* and *N* to *G* (Fig. 8). Because we know that guanine nucleotides (both GTP and GDP) disrupt the stability of the *RG* complex (34), δ must lead to a reduction in the effective affinity of M' (*i.e.* $\delta < 1$). In the model, however, both γJ and M contribute to the value of M'. Thus, to reduce M', the binding of *N* could be negatively coupled either to the state transition ($S_1 \leftrightarrow S_2$) or to the intermolecular association $R \leftrightarrow G$. We reasoned that the correspondence of ligand IA between receptors would be preserved in the first case but not in the second. Based on the effects of GDP shown in Fig. 7*b*, we chose the second option. This means that GDP can change via cooperativity (δ) the stability of the *RG* complex (just like *H* does via α) but cannot directly alter the state transition of the system.

Simulations of Experimental Data—Simulations according to the three model versions were made using a previously described (35, 36) numerical algorithm. The parameters were varied according to the rules discussed above and chosen to best fit the experimental data. The difference in constitutive coupling between DOP and MOP was emulated by increasing J in ACM or γ in ARM and AGM. This is an arbitrary and inconsequent choice, as the values of J and γ can be scaled reciprocally as long as Equations 9–11 are obeyed. For simplification, β was kept constant across ligands in the shown simulations, although we found that small random variations in β could produce similar scatter in the relation of ligand IA between receptors as measured experimentally (Fig. 1*d*). In summary, the sole increase of γ or J in DOP with no change of other parameters can perfectly "fit" the observed phenomenology: the apparent reversal of ligand IA between receptors, disrupted by GDP (Fig. 7); and the uniform decrease of free energy coupling values for ligand and GDP measured in the DOP receptor (Fig. 6).

Relationship with Previous Models—The model presented here is very similar or even mathematically identical (*e.g.* the ARM version in Fig. 8) to previous extensions of the TCM (15, 17, 37). The major difference is the intrinsic state transition, which goes in concert with ligand-induced perturbations in the

extended (15) or cubic (17) ternary complex, but it is opposed by ligands in this model. Consequently, the extended or cubic ternary complex cannot explain the M' and α' covariance discussed here, nor can this model account for the K' and α' covariance observed there. Rather than a contradiction, this indicates that the change in function and change in energy state of the system cannot be described with the same allosteric transition. A more general theoretical framework to interpret the full repertoire of allosteric receptor behavior is needed. BRET studies on constitutively activated receptor mutants are under way in our laboratory and may help us to make a step forward in that direction.

REFERENCES

1. Allen, L. F., Lefkowitz, R. J., Caron, M. G., and Cotecchia, S. (1991) G-protein-coupled receptor genes as protooncogenes: constitutively activating mutation of the alpha 1B-adrenergic receptor enhances mitogenesis and tumorigenicity. *Proc. Natl. Acad. Sci. U.S.A.* **88,** 11354–11358
2. Costa, T., and Herz, A. (1989) Antagonists with negative intrinsic activity at delta opioid receptors coupled to GTP-binding proteins. *Proc. Natl. Acad. Sci. U.S.A.* **86,** 7321–7325
3. Cotecchia, S., Exum, S., Caron, M. G., and Lefkowitz, R. J. (1990) Regions of alpha1-adrenergic receptor involved in coupling to phosphatidylinositol hydrolysis and enhanced sensitivity of biological function. *Proc. Natl. Acad. Sci. U.S.A.* **87,** 2896–2900
4. Kjelsberg, M. A., Cotecchia, S., Ostrowski, J., Caron, M. G., and Lefkowitz, R. J. (1992) Constitutive activation of the alpha 1B-adrenergic receptor by all amino acid substitutions at a single site. Evidence for a region which constrains receptor activation. *J. Biol. Chem.* **267,** 1430–1433
5. Lefkowitz, R. J., Cotecchia, S., Samama, P., and Costa, T. (1993) Constitutive activity of receptors coupled to guanine nucleotide regulatory proteins. *Trends Pharmacol. Sci.* **14,** 303–307
6. Bond, R. A., and Ijzerman, A. P. (2006) Recent developments in constitutive receptor activity and inverse agonism, and their potential for GPCR drug discovery. *Trends Pharmacol. Sci.* **27,** 92–96
7. Costa, T., and Cotecchia, S. (2005) Historical review: negative efficacy and the constitutive activity of G-protein-coupled receptors. *Trends Pharmacol. Sci.* **26,** 618–624
8. Milligan, G. (2003) Constitutive activity and inverse agonists of G protein-coupled receptors: a current perspective. *Mol. Pharmacol.* **64,** 1271–1276
9. Parma, J., Duprez, L., Van Sande, J., Cochaux, P., Gervy, C., Mockel, J., Dumont, J., and Vassart, G. (1993) Somatic mutations in the thyrotropin receptor gene cause hyperfunctioning thyroid adenomas. *Nature* **365,** 649–651
10. Seifert, R., and Wenzel-Seifert, K. (2002) Constitutive activity of G-protein-coupled receptors: cause of disease and common property of wild-type receptors. *Naunyn Schmiedebergs Arch. Pharmacol.* **366,** 381–416
11. Shenker, A., Laue, L., Kosugi, S., Merendino, J. J., Jr., Minegishi, T., and Cutler, G. B., Jr. (1993) A constitutively activating mutation of the luteinizing hormone receptor in familial male precocious puberty. *Nature* **365,** 652–654
12. Smit, M. J., Vischer, H. F., Bakker, R. A., Jongejan, A., Timmerman, H., Pardo, L., and Leurs, R. (2007) Pharmacogenomic and structural analysis of constitutive G protein-coupled receptor activity. *Annu. Rev. Pharmacol. Toxicol.* **47,** 53–87
13. Costa, T., Ogino, Y., Munson, P. J., Onaran, H. O., and Rodbard, D. (1992) Drug efficacy at guanine nucleotide-binding regulatory protein-linked receptors: thermodynamic interpretation of negative antagonism and of receptor activity in the absence of ligand. *Mol. Pharmacol.* **41,** 549–560
14. De Lean, A., Stadel, J. M., and Lefkowitz, R. J. (1980) A ternary complex model explains the agonist-specific binding properties of the adenylate cyclase-coupled beta-adrenergic receptor. *J. Biol. Chem.* **255,** 7108–7117
15. Samama, P., Cotecchia, S., Costa, T., and Lefkowitz, R. J. (1993) A mutation-induced activated state of the beta 2-adrenergic receptor. Extending the ternary complex model. *J. Biol. Chem.* **268,** 4625–4636
16. Weber, G. (1975) Energetics of ligand binding to proteins. *Adv. Protein Chem.* **29,** 1–83
17. Weiss, J. M., Morgan, P. H., Lutz, M. W., and Kenakin, T. P. (1996) The cubic ternary complex receptor-occupancy model I. Model description. *J. Theor. Biol.* **178,** 151–167
18. Wreggett, K. A., and De Léan, A. (1984) The ternary complex model. Its properties and application to ligand interactions with the D2-dopamine receptor of the anterior pituitary gland. *Mol. Pharmacol.* **26,** 214–227
19. Soudijn, W., van Wijngaarden, I., and Ijzerman, A. P. (2005) Structure-activity relationships of inverse agonists for G-protein-coupled receptors. *Med. Res. Rev.* **25,** 398–426
20. Casella, I., Ambrosio, C., Grò, M. C., Molinari, P., and Costa, T. (2011) Divergent agonist selectivity in activating beta1- and beta2-adrenoceptors for G-protein and arrestin coupling. *Biochem. J.* **438,** 191–202
21. Molinari, P., Casella, I., and Costa, T. (2008) Functional complementation of high-efficiency resonance energy transfer: a new tool for the study of protein binding interactions in living cells. *Biochem. J.* **409,** 251–261
22. Molinari, P., Vezzi, V., Sbraccia, M., Grò, C., Riitano, D., Ambrosio, C., Casella, I., and Costa, T. (2010) Morphine-like opiates selectively antagonize receptor-arrestin interactions. *J. Biol. Chem.* **285,** 12522–12535
23. Neilan, C. L., Akil, H., Woods, J. H., and Traynor, J. R. (1999) Constitutive activity of the delta-opioid receptor expressed in C6 glioma cells: identification of non-peptide delta-inverse agonists. *Br. J. Pharmacol.* **128,** 556–562
24. Tryoen-Tóth, P., Décaillot, F. M., Filliol, D., Befort, K., Lazarus, L. H., Schiller, P. W., Schmidhammer, H., and Kieffer, B. L. (2005) Inverse agonism and neutral antagonism at wild-type and constitutively active mutant delta opioid receptors. *J. Pharmacol. Exp. Ther.* **313,** 410–421
25. Salvadori, S., Balboni, G., Guerrini, R., Tomatis, R., Bianchi, C., Bryant, S. D., Cooper, P. S., and Lazarus, L. H. (1997) Evolution of the Dmt-Tic pharmacophore: N-terminal methylated derivatives with extraordinary delta opioid antagonist activity. *J. Med. Chem.* **40,** 3100–3108
26. Balboni, G., Salvadori, S., Guerrini, R., Negri, L., Giannini, E., Bryant, S. D., Jinsmaa, Y., and Lazarus, L. H. (2003) Synthesis and opioid activity of *N*,*N*-dimethyl-Dmt-Tic-NH-CH(*R*)-*R*′ analogues: acquisition of potent delta antagonism. *Bioorg. Med. Chem.* **11,** 5435–5441
27. Balboni, G., Salvadori, S., Guerrini, R., Negri, L., Giannini, E., Bryant, S. D., Jinsmaa, Y., and Lazarus, L. H. (2004) Direct influence of C-terminally substituted amino acids in the Dmt-Tic pharmacophore on delta-opioid receptor selectivity and antagonism. *J. Med. Chem.* **47,** 4066–4071
28. Balboni, G., Guerrini, R., Salvadori, S., Negri, L., Giannini, E., Bryant, S. D., Jinsmaa, Y., and Lazarus, L. H. (2005) Conversion of the potent delta-opioid agonist *H*-Dmt-Tic-NH-CH(2)-Bid into delta-opioid antagonists by *N*(1)-benzimidazole alkylation(1). *J. Med. Chem.* **48,** 8112–8114
29. DeLean, A., Munson, P. J., and Rodbard, D. (1978) Simultaneous analysis of families of sigmoidal curves: application to bioassay, radioligand assay, and physiological dose-response curves. *Am. J. Physiol.* **235,** E97–E102
30. Granier, S., Manglik, A., Kruse, A. C., Kobilka, T. S., Thian, F. S., Weis, W. I., and Kobilka, B. K. (2012) Structure of the delta-opioid receptor bound to naltrindole. *Nature* **485,** 400–404
31. Manglik, A., Kruse, A. C., Kobilka, T. S., Thian, F. S., Mathiesen, J. M., Sunahara, R. K., Pardo, L., Weis, W. I., Kobilka, B. K., and Granier, S. (2012) Crystal structure of the mu-opioid receptor bound to a morphinan antagonist. *Nature* **485,** 321–326
32. Zocher, M., Fung, J. J., Kobilka, B. K., and Müller, D. J. (2012) Ligand-specific interactions modulate kinetic, energetic, and mechanical properties of the human beta2 adrenergic receptor. *Structure* **20,** 1391–1402
33. Weber, G. (1972) Ligand binding and internal equilibria in proteins. *Biochemistry* **11,** 864–878
34. Rasmussen, S. G., DeVree, B. T., Zou, Y., Kruse, A. C., Chung, K. Y., Kobilka, T. S., Thian, F. S., Chae, P. S., Pardon, E., Calinski, D., Mathiesen, J. M., Shah, S. T., Lyons, J. A., Caffrey, M., Gellman, S. H., Steyaert, J., Skiniotis, G., Weis, W. I., Sunahara, R. K., and Kobilka, B. K. (2011) Crystal structure of the beta2 adrenergic receptor-G_s protein complex. *Nature* **477,** 549–555

35. Onaran, H. O., Costa, T., and Rodbard, D. (1993) Beta gamma subunits of guanine nucleotide-binding proteins and regulation of spontaneous receptor activity: thermodynamic model for the interaction between receptors and guanine nucleotide-binding protein subunits. *Mol. Pharmacol.* **43,** 245–256
36. Pradines, J. R., Hasty, J., and Pakdaman, K. (2001) Complex ligand-protein systems: a globally convergent iterative method for the $n \times m$ case. *J. Math. Biol.* **43,** 313–324
37. Kaya, A. I., Ugur, O., Oner, S. S., Bastepe, M., and Onaran, H. O. (2009) Coupling of beta2-adrenoceptors to XLalphas and Galphas: a new insight into ligand-induced G protein activation. *J. Pharmacol. Exp. Ther.* **329,** 350–359